An Efficient Ray Tracing Propagation Simulator for Analyzing Ultrawideband Channels

Gianluigi Tiberi[1], Stefano Bertini[1], Wasim Q. Malik[2], Agostino Monorchio[1], David J. Edwards[2], and Giuliano Manara[1]

[1]Microwave and Radiation Laboratory - Department of Information Engineering, University of Pisa, Via G. Caruso, I-56122 Pisa, Italy. Email: {g.tiberi, stefano.bertini, a.monorchio, g.manara}@iet.unipi.it

[2]Department of Engineering Science, University of Oxford, Parks Road, Oxford, OX1 3PJ, UK. Email: {wasim.malik, david.edwards}@eng.ox.ac.uk

***Abstract*—A fundamental step in ultrawideband (UWB) communication systems involves the characterization of the indoor propagation channel. In this paper, we show that UWB channel parameters can be predicted accurately by ray tracing (RT) simulation carried out at various frequencies over the signal bandwidth. Our RT algorithm is independent of frequency, therefore the determination of the rays reaching a given location is made only once. Moreover, a parallel ray approximation is used to improve significantly the computational efficiency of the RT based approach. The excellent agreement between simulation results and measured data proves that our RT-based tool can be used successfully for accurate and reliable site-planning in UWB systems.**

***Index Terms*—Ray tracing, channel simulation, indoor propagation, ultrawideband.**

I. Introduction

An ultrawideband (UWB) radio signal is characterized by a large fractional bandwidth. The frequency selectivity of the propagation process introduces fundamental differences between UWB channels and conventional (narrowband) channels. Various channel modeling techniques can be used to describe the UWB channel [1]; in particular, it is possible to use statistical modeling based on frequency or time domain measurement campaigns, or deterministic modeling based on simulations. To date, ray tracing (RT) based approaches have been widely used to characterize the indoor channel for narrowband and wideband systems, while only limited attempts have been made to predict the UWB characteristics [2]-[6]. In order to provide accurate site-planning and for extracting the statistics of the channel, RT simulations must be performed for a large number of locations, and this can lead to an unacceptably high computational time. Therefore, a major aim of RT based approaches is the reduction of the computational cost, which is proportional to the number of spatial point where RT is performed.

In this paper, an approach based on the parallel ray approximation is introduced and successfully used to reduce the RT complexity. It allows us to obtain the frequency responses on a spatial grid of points by employing the RT simulation on a coarser spatial grid, through the assumption that points located close together are illuminated by the same number of rays having the same amplitudes but different phases. Moreover, the accuracy and the validity limits of the approximation are verified through the analysis of the error. A measurement campaign has been conducted to validate the propagation simulator. The excellent agreement between simulation results and measured data proves that the RT based tool can be successfully used for accurate and reliable site planning in UWB systems. As an alternative, it can also be employed for developing statistical propagation models. In this context, it has to be pointed out that, in contrast to measurements, RT allows detailed signal and environment specification; therefore it can facilitate more comprehensive channel characterization, with the additional benefit of efficiency and convenience.

II. Ray-Tracing Analysis

The radio channel experienced at a receiver's location, $\mathbf{u}_n = (x_n, y_n, z_n)$, in a given environment is modeled as a time-invariant linear filter with location-dependent impulse response, $h(t, \mathbf{u}_n)$. The impulse response provides the characterization of the propagation channel and contains the necessary information to analyze any type of signal transmission over that channel.

In a typical wireless channel, the signal arriving at the receiver consists of several multipath components, each resulting from the interaction between the transmitted signal and the surrounding environment. If we assume that the channel features do not vary over the signal bandwidth, B, then the channel frequency response $H(f, \mathbf{u}_n)$, i.e. the Fourier transform (FT) of $h(t, \mathbf{u}_n)$, has constant amplitude and linear phase response [7]. However, this assumption holds true only as far as narrowband signals are concerned, but loses accuracy as the signal bandwidth grows, since the channel behavior is actually determined by frequency-dependent phenomena occurring in the environment, such as reflection, transmission and scattering. The calculation of the frequency response is a key point for UWB channel modeling. In this

section the frequency response will be derived through the RT procedure, while in the next section it will be obtained through measurements. It has to be pointed out that if the channel is considered to be inclusive of the antenna pair, the angular-frequency distortion introduced by UWB antennas must also be taken into account [11].

Let us consider now a transmitted signal, $s(t)$, whose spectrum, $S(f)$, is sampled over the band B at the frequencies $[f_1,....,f_{nf}]$, where *nf* is the number of discrete frequency points. The samples of the spectrum, $R(f,\mathbf{u}_n)$, of the received signal, $r(t,\mathbf{u}_n)$, are thus given by:

$$R(f_k,\mathbf{u}_n) = S(f_k)H(f_k,\mathbf{u}_n) \quad \text{for } k=\{1,2,..,nf\}. \quad (1)$$

The samples of the channel's frequency response $H(f_k,\mathbf{u}_n)$ can be obtained as the ratio of the received samples, $R(f_k,\mathbf{u}_n)$, to the transmitted samples, $S(f_k)$. Then, an inverse discrete Fourier transform (IDFT) provides the sampled version of $h(t,\mathbf{u}_n)$. In our approach, the samples of the frequency response, $H(f_k,\mathbf{u}_n)$, can be determined by employing an RT simulator [7], where the signal source is a set of dipoles transmitting continuous wave (CW) carriers at the frequencies f_k.

The RT tool "EMvironment 3.0" used in this study is an efficient three-dimensional (3-D) simulator based upon a combination of binary space partition and image theory derived from Computer Graphics, and was developed at the Microwave and Radiation Laboratory of the University of Pisa, Italy. Firstly, ray paths are identified; then complex vector electromagnetic field components are evaluated in terms of plane waves undergoing multiple phenomena of reflection, transmission and diffraction. The reflected field is evaluated through geometrical optics (GO), where the number of rays depends on the maximum order of the bouncing allowed, which is set a priori. Moreover, first-order diffractions from the edges are evaluated through heuristic uniform theory of diffraction (UTD) dyadic diffraction coefficients, valid for discontinuities in impedance surfaces. Transmissions through walls and objects are evaluated by resorting to a multilayered media description.

Apparently, the procedure described above can be highly CPU-intensive, depending on the number, *nf*, of frequency samples. However, it is worthwhile remarking that the time-consuming part in the RT algorithm is the determination of the rays reaching a given location. This can be made only once at the beginning of the procedure, since the algorithm is frequency independent. The low-complexity calculation of the received signal is then repeated *nf* times.

To provide accurate site planning for realistic indoor environments and to extract the channel statistics, the frequency response has to be calculated for a large amount of points. The computational cost of RT-based tools is linearly proportional to the number of spatial point where it is performed; therefore it would be desirable to avoid, when possible, this brute-force procedure [8]. Next, an approach based on the parallel ray approximation is introduced. It allows us to obtain the frequency responses on the spatial grid of points by employing the RT simulation on a coarser spatial grid, through the assumption that points located nearby are reached by the same number of rays having same amplitudes but different phases.

In this respect, let us consider a location, $\mathbf{u}_n$, and assume that RT has been performed for $\mathbf{u}_n$, so that the frequency response, $H(f,\mathbf{u}_n)$, and therefore the impulse response, $h(t,\mathbf{u}_n)$, are known. Denoting with N_n^{rays} the number of rays reaching $\mathbf{u}_n$, it holds that:

$$H(f,\mathbf{u}_n) = \sum_{i=1}^{N_n^{rays}} H_i(f,\mathbf{u}_n), \quad (2)$$

where $H_i(f,\mathbf{u}_n)$ are the frequency responses for the i^{th} ray. If $\mathbf{u}_m$ is located near $\mathbf{u}_n$, and $\mathbf{u}_n$ is not in a transition from a lit to a shadow region, it is reasonable to assume that the variations of number and magnitude of multipath components reaching $\mathbf{u}_m$ with respect to $\mathbf{u}_n$ are negligible. Therefore, the multipath components reaching $\mathbf{u}_m$ can be simply obtained by a proper phase shift of the multipath components reaching $\mathbf{u}_n$. The phase shifts are calculated by evaluating the path length differences obtained by projecting the distances $\mathbf{d}_{n,m} = \mathbf{u}_n - \mathbf{u}_m$ on the unit vectors $\mathbf{v}_i$, which define the multipath components. Therefore, we obtain:

$$H(f,\mathbf{u}_m) \approx \sum_{i=1}^{N_n^{rays}} H_i(f,\mathbf{u}_n) e^{j2\pi\frac{f}{c}\mathbf{d}_{n,m}\cdot\mathbf{v}_i}. \quad (3)$$

The inverse discrete Fourier transform (IDFT) then provides the sampled version of $h(t,\mathbf{u}_m)$.

The proposed approach allows an analytical synthesis of $h(t,\mathbf{u}_m)$, avoiding a new RT simulation. The accuracy and the limit of validity of the procedure are evaluated by calculating the error between the analytically synthesized and the RT derived impulse responses, a method not usually adopted when applying the parallel ray approximation. Moreover, it is worthwhile mentioning that the procedure is site-specific since it resorts to site-specific information contained in the unit vectors of the multipath components reaching $\mathbf{u}_n$, while in other, more conventional approaches, phase shifts are usually considered uniformly distributed random variables [9].

III. Channel Measurements

Frequency-domain UWB channel measurements were conducted in a typical indoor environment, consisting of a 5 m×4.7 m×2.6 m laboratory of the Communications Research Group at the University of Oxford, with block walls, concrete floors and ceiling, a large glass window, a wooden door, metallic and wooden furniture (benches, tables, shelves), as shown in Fig. 1(a). A vector network analyzer (VNA) arrangement was used to sound the channel at 1601 discrete

frequencies in the FCC UWB band $[f_l, f_h]$, where $f_l = 3.1$ GHz and $f_h = 10.6$ GHz [10]. The measurement bandwidth was thus B=7.5 GHz. The entire measurement system was calibrated to remove the frequency-dependent attenuation and phase distortion.

A pair of vertically polarized discone antennas was used to conduct the measurements [11]. The location of the transmitting antenna was fixed, while the receiver antenna was stationed atop a computer-controlled horizontal position grid with dimensions 0.5 m×0.5 m and resolution 1 cm×1 cm, leading to a 50×50 measurement points grid. Both the line-of-sight (LoS) and the non-line-of-sight (NLoS) cases were considered. A careful adjustment was undertaken for both antennas to be exactly at the same height and in vertical position to avoid any polarization mismatch. For each receiver location, the discrete complex frequency transfer function was recorded.

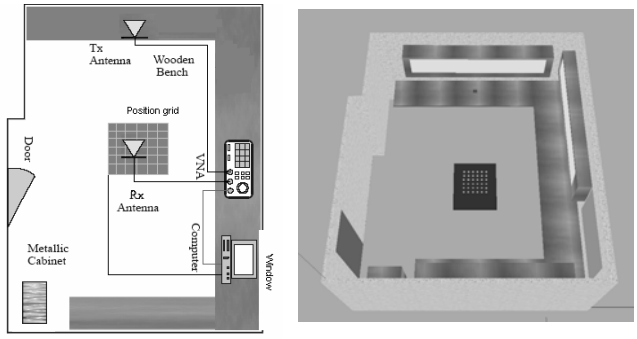

(a) (b)

Fig. 1. (a) A plan view of the measurement environment, LoS case: the room is 5m×4.7m×2.6m, the transmitter (Tx) and the receivers are located at the same height of 1.35 m; (b) Pictorial view of the RT reconstructed scenario (ceiling not shown), LoS case; the transmitter and the receivers (white dots grid) are also shown.

IV. Numerical Results

The scenario has been reconstructed in the RT simulator as shown in Fig. 1(b). Particular care has been used for including windows, doors and furniture with appropriate electrical properties, as summarized in Table I. We have assumed in this study that the electrical properties do not depend appreciably on the frequency; however a pronounced variation of the electrical properties with frequency can be easily taken into account using this technique. A spatial grid of 50×50 points was placed over the same 0.5 m×0.5 m area which was used for the measurements. The number of bouncing rays has been set to 4 for the LoS case and to 5 for NLoS cases after a detailed investigation of the convergence of the simulation results. Moreover, the frequency dependent radiation pattern of the discone antenna has been applied at both the transmitter and the receiver. Note that this can be easily done since in the RT simulation the angle of departure (AoD) and the angle of arrival (AoA) are known. For each grid point, the frequency response can be determined by employing the RT simulator [12], where the signal source is a set of dipoles transmitting continuous wave (CW) carriers at the same $nf = 1601$ frequencies as employed by the VNA. The NLoS case is created by reproducing the measurement procedure, i.e. by positioning an absorbing plane between the transmitter and the receivers.

The parallel ray based approach permits a dramatic reduction in the computational cost of the RT based tool, since it allow us to obtain the frequency responses on a spatial grid by employing the RT simulation on a coarser spatial grid. The error check provides a criterion for the choice of the coarser spatial grid where the RT is performed. Referring to the scenario given in Section III where a spatial grid of 50×50 points is defined, the 50×50 frequency responses have been calculated by employing the RT simulation on a spatial grid of 10×10 points only. The computational time for the RT simulation depends on the complexity of the reconstructed scenario, the number of bouncing rays included and the number of spatial points. For the RT simulation described in this paper, the total computational time is approximately 12 hours on a 2.4 GHz Pentium IV computer with 1 GB RAM. Note that this computational time is obtained when the afore-mentioned parallel ray approximation is adopted, while it grows up to 32 hours for the conventional RT procedure (see Table II). The parallel ray approximation thus permits a time reduction to approximately 38%. Finally, it is worth pointing out that other approaches for modeling indoor wideband propagation channels are usually based on FDTD methods. However, although they are rigorous and also applicable to complex inhomogeneous dielectric structures, they turn out to be much more time-consuming and CPU-intensive.

TABLE I
Material Characteristics

Material	**σ [S/m]**	**ε_r**	**Thickness[cm]**
ceiling (concrete)	0.01	9	15.0
floor (concrete)	0.01	9	-
internal wall (concrete)	0.01	9	7.5
external wall (concrete)	0.01	9	15.0
benches, door, table (wood)	10^{-5}	13	3.0
window (glass)	10^{-12}	7.6	3.0

TABLE II
COMPUTATIONAL TIME COMPARISON

	Conventional RT	**Parallel Ray Approx**
Time (h)	32h	12h
Saved Time (%)	-	62.5%

A. Power Delay Profile Analysis

Next, from each of the 50×50 frequency responses, the impulse response is derived through the IDFT, the propagation delay is removed, and a spatial average is calculated to obtain the power delay profile PDP. The RT derived PDP has been compared with the measured PDP.

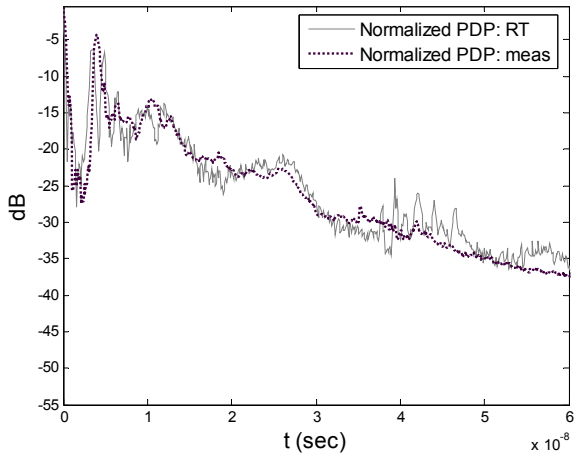

Fig. 2. Comparison of the PDPs, LoS case (measured and simulated). The abscissa represents the time exceeding that of the first arrived ray.

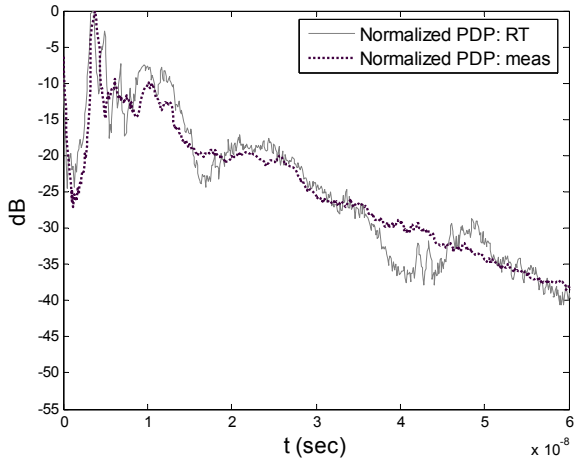

Fig. 3. Comparison of the PDPs, NLoS case (measured and simulated). The abscissa represents the time exceeding that of the first arrived ray.

In Fig. 2, the measured normalized PDP and the normalized PDP calculated through the RT procedure are plotted for the LoS case. The two curves show good agreement. A check on the correlation coefficient between the two curves has been performed, leading to a value of 0.85. Some differences can be observed in the 40 ns region: these differences are presumably due to an imperfect reconstruction of the scenario in terms of furniture and dielectric properties of the materials. Indeed, it can be shown that the RT derived PDP is sensitive to these scenario features, while it is robust towards the reconstruction of the scenario in terms of its dimensions. Fig. 3 refers to the NLoS case; also in this case a good match between the curves can be observed.

A. Angle of Arrival Analysis

In this sub-section, AoAs will be analyzed with the purpose of showing the capability of the RT based procedure for developing statistical UWB propagation models. A similar approach can be applied for statistical modeling of other quantities such as delay, AoD, times of arrival.

Referring to the AoAs, let us consider again the location $\mathbf{u}_n$ and let us assume that RT has been performed for $\mathbf{u}_n$, so that $H(f,\mathbf{u}_n)$ and therefore $h(t,\mathbf{u}_n)$ are known. Denoting by N_n^{rays} the number of rays reaching $\mathbf{u}_n$, it holds that:

$$h(t,\mathbf{u}_n)=\sum_{i=1}^{N_n^{rays}} h_i(t,\mathbf{u}_n), \tag{4}$$

$$h_i(t,\mathbf{u}_n)=\int_B H_i(f,\mathbf{u}_n)e^{j2\pi f}df. \tag{5}$$

Here, $H_i(f,\mathbf{u}_n)$ and $h_i(t,\mathbf{u}_n)$ are the frequency and impulse responses of the i^{th} ray. For each ray, RT provides the AoAs for both elevation and azimuth planes, denoted by (θ_i,ϕ_i). Next, a cutoff threshold of –30 dB below the strongest ray is applied to ensure that only effective paths are modeled. This procedure is required since in RT the paths are determined in a purely geometrical way; conversely, here only the AoAs of the dominant paths are taken into account for the statistical characterization. Therefore, the power associated with each ray is calculated, and rays with power less than –30 dB below the strongest path are not considered.

It should be noted that the impulse response of the i^{th} ray, and consequently, the associated power, is calculated from (5) by integrating over the band *B*. In order to highlight the effect of the frequency on the AoAs, we can instead divide the band *B* in a number of sub-bands and then perform the integration in (5) over the sub-bands separately. The set of rays reaching a single location will then potentially change with frequency, and the AoA statistics may exhibit frequency dependence.

Fig. 4 shows the probability density function (pdf) of the azimuthal AoAs for the LoS case, when considering two distinct sub-bands (3.1 - 4.85 GHz and 6.2 - 9.7 GHz) with a threshold of -30 dB. Some differences can be noted between

the pdfs of the two sub-bands, and this highlights the impact of frequency on channel statistics.

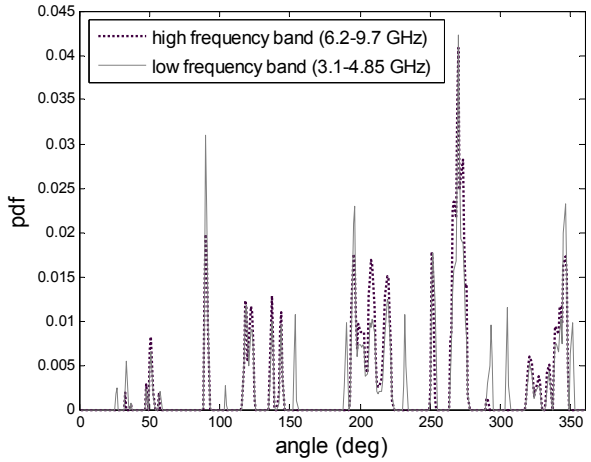

Fig. 4. Probability density function (pdf) of azimuthal AoAs when considering two distinct sub-bands (3.1-4.85 GHz and 6.2-9.7 GHz). The pdfs have been derived numerically by RT.

From Fig. 4, it is possible to visually define a number of clusters. Some propagation studies for UWB channels have reported that clustering can be observed in both the temporal and angular domains [13]. In our context, "clusters" are a group of multipath components showing similar AoAs. Then, the pdf of the AoAs with respect to the cluster mean, i. e. the intracluster arrival, has been derived and compared to the Laplacian distribution [13],[14]:

$$f(\phi) = \frac{1}{\sqrt{2}\sigma_\phi} e^{-\sqrt{2}\frac{|\phi|}{\sigma_\phi}}. \quad (6)$$

A Chi-square fitness test has been performed for both the low-band and high-band case, and the parameter $\sigma_\phi = 10^\circ$ and $\sigma_\phi = 12^\circ$ have been found. Fig. 5 shows the pdf of azimuthal AoAs with respect to the cluster means when considering the low frequency sub-band (3.1-4.85 GHz). Note that the RT derived parameters are very similar to those given in [14], where the same measured data used in this paper have been processed to extract the angular statistics, obtaining $\sigma_\phi = 11^\circ$ and $\sigma_\phi = 14^\circ$ for the low and high sub-band, respectively.

V. Conclusion

We have presented an efficient procedure based on a RT method for analyzing UWB indoor channel. The RT simulations are carried out at different frequencies over the signal bandwidth and the impulse response is then extracted. To this end, it is important to note that the RT algorithm is independent of frequency, therefore the determination of the rays reaching a given location is made only once. Moreover, a parallel ray approximation, usually adopted in array analysis, is successfully used to dramatically reduce the computational time. An excellent agreement with measurements is achieved, demonstrating the effectiveness of such a method for accurate site-planning in realistic indoor environments. As an alternative, it can be employed for developing statistical propagation models. Using this tool, the impact of the frequency on the AoA statistics of UWB channels has been highlighted.

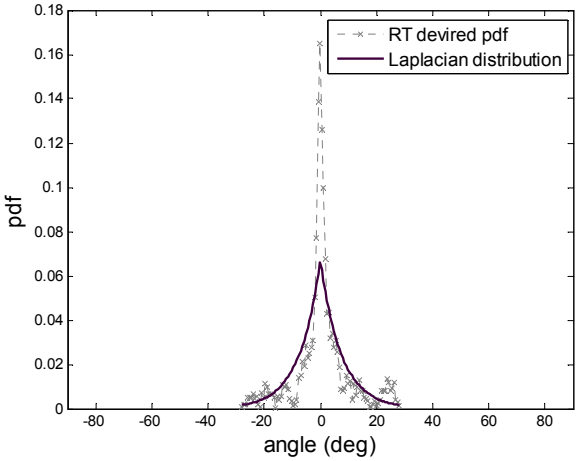

Fig. 5. Probability density function of azimuthal AoAs with respect to the cluster means when considering the low frequency sub-band (3.1-4.85 GHz). The dotted line represents the pdf which has been derived numerically by using the RT derived data; the continuous line represents the best fit Laplacian density distribution.

References

[1] A. F. Molisch, "Ultrawideband propagation channels - theory, measurement and modeling", *IEEE Trans. Veh. Technol.*, vol. 54, no. 5, Sept 2005, pp 1528-1545.

[2] F. Tehoffo-Talom, B. Uguen, E. Plouhinec, G. Chassay, "A site-specific tool for UWB channel modeling", *Proc. Int. Workshop UWB Sys. Tech.*, May 2004

[3] H. Sugahara, Y. Watanabe, T. Ono, K. Okanoue, and S. Yarnazaki, "Development and experimental evaluations of 'RS-2000' - a propagation simulator for UWB systems," in *Proc. IEEE Int. Workshop Ultra Wideband Sys. joint with Conf. Ultra Wideband Sys. Tech*. Kyoto, Japan, May 2004.

[4] A. M. Attiya and A. Safaai-Jazi, "Simulation of ultra-wideband indoor propagation," *Microwave Opt. Tech. Lett*., vol. 42, July 2004.

[5] Y. Zhang, A. K. Brown, "Ultra-wide bandwidth communication channel analysis using 3-D ray tracing", *Proc. Int. Symp. Wireless Comm. Sys.*, Sept. 2004

[6] W. Q. Malik, C. J. Stevens, and D. J. Edwards, "Spatio-temporal ultrawideband indoor propagation modelling by reduced complexity geometric optics," to appear in *IET Commun*.

[7] M. F. Catedra, J. P. Arriaga, *Cell Planning for Wireless Communications*, Artech House, 1999.

[8] K. H. Ng, E. K. Tameh, A. R. Nix, "Modeling and performance prediction for multiple antenna systems using enhanced ray tracing", *Proc. IEEE Wireless Comm. Networking Conf*., March 2005

[9] A. F. Molisch, M. Steinbauer, M. Toeltsch, E. Bonek, R. S. Thomä, "Capacity of MIMO systems based on measured wireless channel", *IEEE J. Select. Areas Commun*., vol. 20, no. 3, April 2002, pp. 561-569

[10] A. M. Street, L. Lukama, D. J. Edwards, "Use of VNAs for wideband propagation measurements", *IEE Proc.–Commun.,* vol 148, no. 6, Dec. 2001, pp 411 – 415

[11] W. Q. Malik, D. J. Edwards, and C. J. Stevens, "Angular-spectral antenna effects in ultrawideband communications links," *IEE Proc.–Commun*., vol. 153, no. 1, Feb. 2006.

[12] G. Tiberi, S. Bertini, A. Monorchio, F. Giannetti, G. Manara, "Modeling realistic wide-band indoor propagation channels by using an efficient ray-tracing simulator", *Proc. IEEE Antennas Propagat. Soc. Int. Symp.*, July 2006

[13] R. Jean-Marc Cramer, Robert A. Scholtz, and Moe Z. Win, "Evaluation of an Ultra-Wide-Band Propagation Channel", *IEEE Trans. Antennas Propagat*., vol. 50, no. 5, May 2002, pp 561-570

[14] Y. Zhang, A. K. Brown, W. Q. Malik, and D. J. Edwards, "High resolution 3-D angle of arrival determination for indoor UWB multipath propagation", to appear in *IEEE Trans. Wireless Commun.*